Journal of Nuclear Materials 307–311 (2002) 229–235
journal of nuclear materials
www.elsevier.com/locate/jnucmat

Evolution of the mechanical properties and microstructure of ferritic–martensitic steels irradiated in the BOR-60 reactor

V.K. Shamardin *, V.N. Golovanov, T.M. Bulanova, A.V. Povstyanko, A.E. Fedoseev, Z.E. Ostrovsky, Yu.D. Goncharenko

SSC RF Research Institute of Atomic Reactors, Ulyanovsk region, 433510 Dimitrovgrad, Russia

Abstract

The effect of neutron irradiation on mechanical properties of low-activation ferritic–martensitic (FM) steels 0.1C–9Cr–1W, V, Ta, B and 0.1C–12Cr–2W, V, Ti, B is studied under tension at temperatures of 330–540 °C and doses of 50 dpa. Steel 0.1C–13Cr–Mo, V, Nb, B was chosen for comparison. At irradiation temperatures of 330–340 °C, the radiation hardening of steel with 9%Cr achieves saturation at a dose of 10 dpa. In this case as compared to steels with 12%Cr, the fracture surface is characterized as ductile without cleavage traces. At irradiation temperatures higher than 420 °C, there is no difference in the behavior of the materials under investigation. The data on radiation creep obtained by direct measurement and from the profilometry data satisfy a model $\bar{\varepsilon}/\bar{\sigma} = B_0 + D\dot{S}$, when B_0 and D have the values typical for steels of FM type.

1. Introduction

Investigation of low activation ferritic–martensitic (FM) steels is the high priority task in the programs on the development of structural materials for the first wall and blanket of the demonstration fusion reactor DEMO. The countries belonging to the European Community, Japan, USA and Russia carry out systematic development and research in this field. At present the most promising steel compositions (9–12%Cr) alloyed with tungsten, vanadium and tantalum (excluding molybdenum, niobium and some other elements, which form long-lived isotopes under irradiation, from steel compositions) have been chosen. It was revealed that as a result of irradiation, steels with 9%Cr (martensitic structure) have a less pronounced shift of the brittle-to-ductile transition temperature than those with 12%Cr (FM structure) [1,2]. An important recent result is the experimental fact [3] that the brittle-to-ductile transition temperature of steels 0.1%C–9%Cr–2W–V, Ta remains below room temperature after irradiation up to 60 dpa ($T_{irr} \approx 390$–600 °C). Paper [4] indicates a specific role of tantalum added into solid solution for to provide good ductility at high doses.

The objective of the present paper is to study the effect of high-dose neutron irradiation on the properties of steels 0.1C–9Cr–1W–V, Ta, B and 0.1C–12Cr–2W–V, Ti, B developed in Russia and to provide additional information for optimization of structural materials for the future fusion reactors.

2. Methods of the experiment performance and irradiation conditions

The following steels have been investigated: 0.1%C–9%Cr–1%W–V, Ta, B; 0.1%C–12%Cr–2%W–V, Ti, B; 0.1%C–13%Cr–2%Mo–V, Nb, B.

The detailed composition and thermal treatment of the steels are described in paper [5]. Fig. 1 shows dose and temperature irradiation parameters of the BOR-60 experimental assembly, i.e. a hexagonal tube with the maximum across-flats dimensions 44 × 1 mm was made

* Corresponding author. Tel.: +7-84235 3 2021; fax: +7-84235 3 5648.
E-mail address: fae@niiar.ru (V.K. Shamardin).

0022-3115/02/$ - see front matter
PII: S0022-3115(02)01179-0

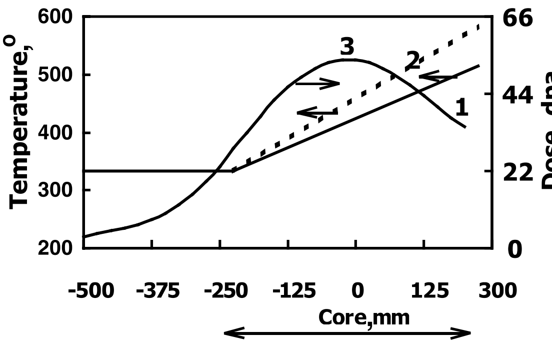

Fig. 1. Temperature and dose distribution as a function of core height under irradiation in the BOR-60 experimental assembly: 1 – wrapper made of steel 0.1C–9Cr–1W, V, Ta, B; 2 – specimens of steel 0.1C–12Cr–2W, V, Ti, B; 3 – damage dose, dpa.

of steel 0.1%C–9%Cr–1%W–V, Ta, B. This assembly included 18 fuel elements and one tube ∅ 6.9 × 0.4 mm where five-fold tensile test specimens of steel 0.1%C–12%Cr–2%W–V, Ti, B having 3 mm gauge diameter were irradiated. The assembly was irradiated in rows 4 and 2 of the BOR-60 core for 3 years.

Profilometry of the hexagonal tube made of steel 0.1%C–9%Cr–1%W–V, Ta, B was performed to evaluate the radiation creep modulus and swelling values. The across-flats dimension (deformation between opposite sides ΔD) from the measurement of three pairs of sides and the diagonal dimensions ΔS were determined.

The creep modulus was defined from the relationship [6]:

$$\Delta D = B_0 P K t G, \quad (1)$$

where B_0 is creep modulus – $\mathrm{MPa^{-1}\,dpa^{-1}}$; P is the sodium pressure at the facility inlet – ≈0.5 Mpa; Kt is the damage dose; G is a geometric factor – 2.2×10^4 mm.

Assuming that the change of the hexagonal tube diagonals (ΔS) can be attributed to swelling phenomenon, the following relationship was used:

$$\frac{\Delta S}{S} = \frac{1}{3}\frac{\Delta V}{V}, \quad (2)$$

where $\Delta V/V$ is the steel swelling value at corresponding values of damage dose and irradiation temperature (Fig. 1).

The radiation creep strain of the hexagonal tube was defined from the relationship

$$\varepsilon_{\mathrm{creep}} = \left[\left(\frac{\Delta D}{2}\right) - \varepsilon_{\mathrm{swelling}}\right]. \quad (3)$$

For internally pressurized tubes made of steel 0.1%C–13%Cr-2%Mo–V, Nb, B swelling was defined from the TEM examinations data and the radiation creep component was defined from the following relationship:

$$\left(\frac{\Delta d}{d}\right)_{\mathrm{irr}}^{\mathrm{creep}} = \frac{\Delta d}{d} - \frac{1}{3}\frac{\Delta V}{V}, \quad (4)$$

where $\Delta d/d$ is the irradiation induced diameter change of the internally pressurized tubes.

The tensile test methods and structural investigations by means of TEM are described in paper [5].

3. Experimental results

3.1. Mechanical property date

Fig. 2 gives a summary of the dose dependencies of radiation hardening and relative elongation of steels 0.1C–9Cr–1W–V, Ta, B at the irradiation temperature of 335 °C. Saturation of radiation hardening above 10 dpa below 400 °C was observed [3]. Evaluation of the dislocation loop density in steel 0.1C–9Cr–1W, V, Ta, B from TEM data indicated a very high concentration of $1.4–4.5 \times 10^{16}\ \mathrm{cm^{-3}}$ with sizes from 7.5 to 14.0 nm (at 335 °C, ≃15–20 dpa).

The reduction in values of total and uniform elongation are at levels typical for this category of materials after irradiation at 320–350 °C [5].

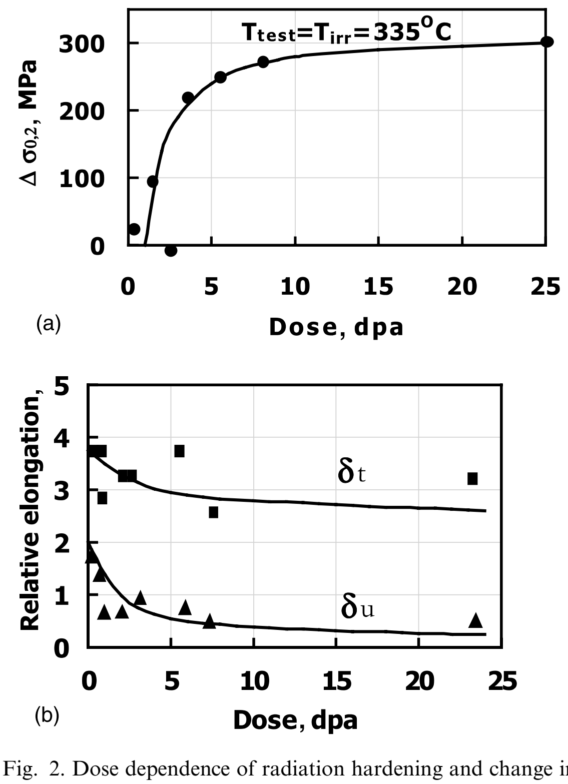

Fig. 2. Dose dependence of radiation hardening and change in the relative elongation of steel 0.1C–9Cr–1W, V, Ta, B at $T_{\mathrm{irr}} \simeq 335$ °C.

Fig. 3 presents the temperature dependencies of yield strength and relative elongation of irradiated steels 0.1C–9Cr-1W–V, Ta, B and 0.1C–12Cr–2W, Ti, V, B in comparison with steel 0.1C–13Cr–2Mo, V, Nb, B. These dependencies characterize the reduction of radiation hardening with increasing irradiation temperature. Recovery of ductility (Fig. 3(a)) for steel 0.1C–9Cr–1W, V, Ta, B begins at temperatures close to 380 °C.

In the plastic strain localization region, tensile stress–strain diagrams (Fig. 4(a)) of irradiated steel 0.1C–9Cr–1W–V, Ta, B show serrations that are most pronounced at a temperature of about 350 °C and which actually disappear at a test temperature of 430 °C. As the experiments indicate, with increasing test temperature the yield strength of the steel decreases by a factor of two (Fig. 3). According to a hypothesis by Klueh [7,8], the good ductile properties of steels 0.1C–9Cr–2W, V, Ta, B are caused by the fact that more than 90% of the Ta is in solid solution and therefore increases fracture stress and provides a low brittle-to-ductile transition temperature in the unirradiated state and only a small shift as a result of irradiation. In our opinion, detection of dynamic strain aging within the irradiation and test temperature range 335–430 °C proves the fact that radiation-accelerated processes of precipitates formation (obviously with tantalum participation) take place that influence the irradiated steel failure mechanism.

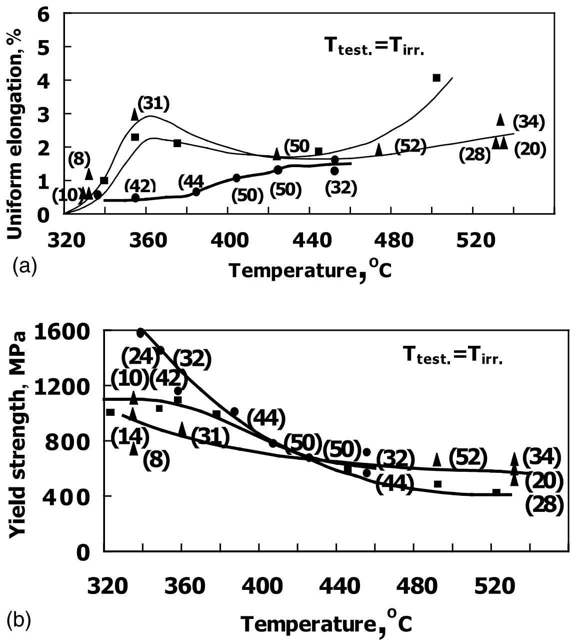

Fig. 3. Uniform relative elongation (a) and temperature dependence of the yield strength (b) of steels 0.1C–9Cr–1W, V, Ta, B (●); 0.1C–12Cr–2W, V, Ti, B (■) and 0.1C–13Cr–2Mo, V, Nb, B (▲), dose values are indicated in brackets.

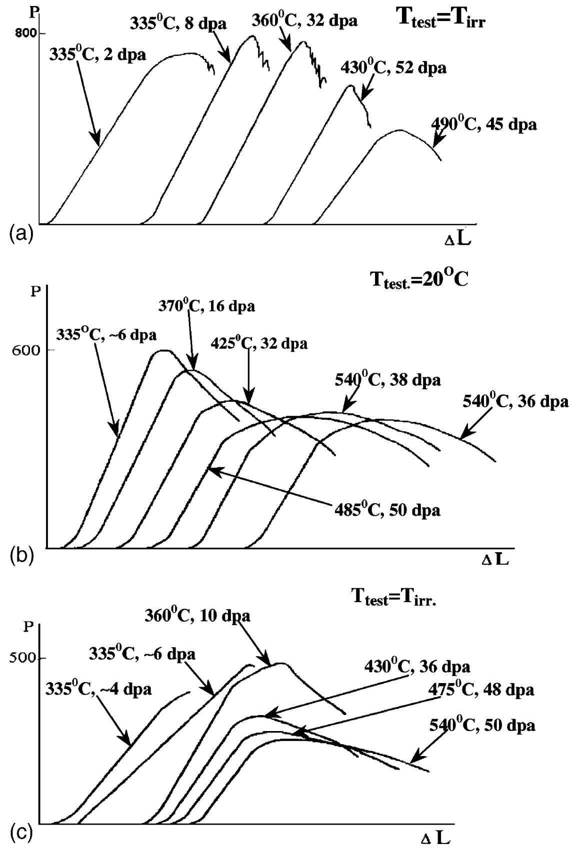

Fig. 4. Typical tensile stress–strain diagrams for irradiated FM steels: (a) steel 0.1C–9Cr–1W, V, Ta, B ($T_{test} = T_{irr}$); and (b), (c) steel 0.1C–12Cr–2W, V, Ti, B: $T_{test} = 20$ °C, ($T_{test} = T_{irr}$) respectively.

Fig. 5(a) and (b) show the failure mode at temperatures 335 and 430 °C. In both cases, the failure is ductile and intragranular. The failure is initiated by plastic strain at precipitates with a maximum size up to 1–2 μm. One should not exclude the presence of smaller particles in the small-size holes. The formation of smaller particles can be caused by a long-term (for more than 3 years) radiation-thermal effect that has changed the initial microstructure.

Fig. 4(b) and (c) provide tensile diagrams for steel 0.1C–12Cr–2W, V, Ti, B. It is evident that under comparable irradiation conditions (335 °C and 6–12 dpa), steel with 12%Cr, as compared to steel 0.1C–9Cr–1W, Ta, V, B, actually loses the ability for strain hardening accompanied by a sharp reduction in strain before neck formation (Fig. 4(b) – the diagram for $T_{test} \approx 20$ °C). At $T_{test} = T_{irr} = 335$ °C (Fig. 4(c)) the neck formation strain is $\leqslant 1\%$. In this case, Frank loops and small voids dominate the microstructure [9]. Failure has a quasi-cleavage appearance (Fig. 5(c) and (d)) with local flat regions present in the fracture. At irradiation and test

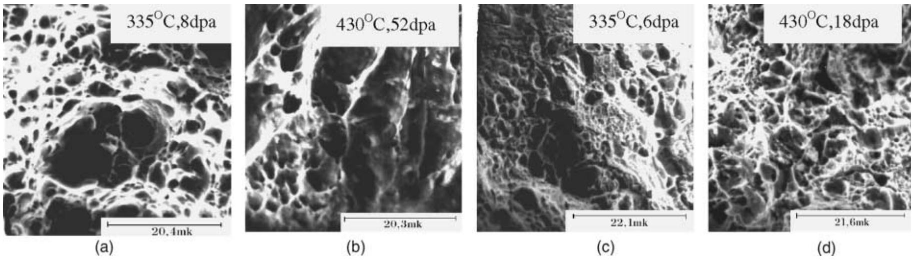

Fig. 5. Typical SEM fractographs of the failure surface of tensile speciments of irradiated steels 0.1C–9Cr–1W, V, Ta, B (a), (b) and 0.15C–12Cr–2W, V, Ti, B (c), (d).

temperatures above 360 °C (Figs. 3 and 4) the steel microstructure suffers essential changes and the strain before necking increases sharply.

Temperature- and dose-induced changes in the uniform elongation of steel 0.1C–12Cr–2W, V, Ti, B following irradiation (Fig. 3(a)) are in good agreement with the results obtained with steel 0.1C–13Cr–2Mo, V, Nb, B within comparable dose-temperature intervals. At the same time in the irradiation and test temperature range 335–430 °C steel 0.1C–9Cr–1W, V, Ta, B show greater radiation hardening, $\Delta\sigma_{0.2}$, and reduced uniform elongation in comparison with steel 0.1C–12Cr–2W, V, Ti, B. According to [8] this can be explained by the presence of tantalum in steel 0.1C–9Cr–1W, V, Ta, B, and by its retention in the solid solution within the specified damage dose interval to 50 dpa and up to $\simeq$430 °C. Serrations in the stress–strain curves disappear (Fig. 4(a)).

Tensile experiments do not provide a direct answer to the question how the brittle-to-ductile temperature shift of steel 0.1C–9Cr–1W, V, Ta, B will change after irradiation up to 50 dpa dose at irradiation temperatures ranging from 335 to 430 °C. A proportional increase in $\Delta\sigma_y$ and shift ΔT is expected [10] in the case the irradiation temperatures below 425 °C and the radiation-induced recovery of the martensitic structure accompanied by the formation of secondary phases of relatively great size does not occur. The increase of irradiation temperature in the range 350–450 °C does not lead to a recovery of the brittle-to-ductile transition temperature for steel 0.1C–9Cr–2W, V, Ta [8]; on the contrary, the shift increases. As already mentioned, this is related to tantalum release from the solid solution. In summary, the results obtained from, the tensile tests do not contradict the published data for steels of 0.1C–9Cr–2W, V, Ta type but complement them.

3.2. Swelling and radiation creep

The microstructure of irradiated steel 0.1C–13Cr–2Mo–Nb, V, B was investigated. Prior to irradiation in the tempered state, the structure represents a mixture of products as a result of martensite recovery and delta ferritic phase at a ratio of 1:1. Irradiation to a dose of 140 dpa in the temperature range 420–460 °C leads to the formation of voids, a dislocation network and precipitation of a fine-dispersion of radiation-enhanced α'-phase (Fig. 6, Table 1). Cavities were detected in the temperature range 420–460 °C, both in ferrite and tempered martensite (sorbite) grains. Sorbite had a larger average pore size at a lower concentration as compared to δ-ferrite that results in lower swelling in sorbite.

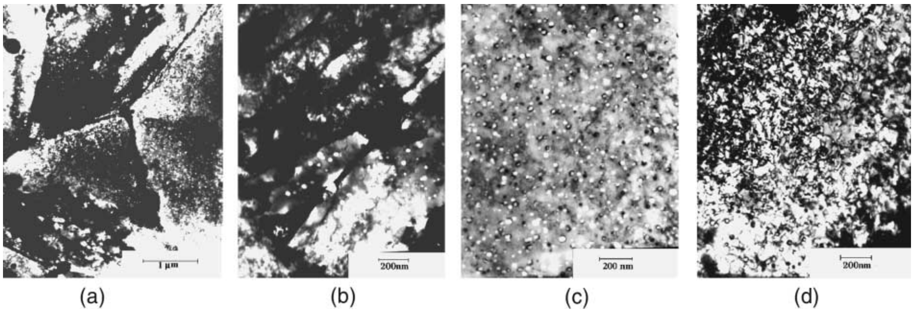

Fig. 6. 0.1C–13Cr–2Mo, V, Nb, B steel microstructures after irradiation to 110 dpa at $T_{irr} = 440$ °C: (a) ferrite and sorbite (general view), ×15 000; (b) dislocation structure, voids and the fine-dispersion phase in sorbite, ×40 000; (c) voids and fine-dispersion phase in ferrite, ×40 000; (d) ferrite dislocation structure, ×40 000.

Table 1
Microstructural parameters of 0.1C–13Cr–2Mo, Nb, V, B steel irradiated to high doses

T_{irr} (°C)		Dose K_t (dpa)	Voids $\bar{d}$ (nm)	V ($\times 10^{-18}$ cm^{-3})	ρ ($\times 10^{-15}$ cm^{-3})	s (%)	α′-phase $\bar{d}_p$ (nm)	ρ_p ($\times 10^{16}$ cm^{-3})	Trait-phase $\bar{d}_p$ (nm)	ρ_p (cm^{-3})	χ-phase $\bar{d}_p$ (nm)	ρ_p (cm^{-3})
350–380	F[a]	~140	8.2	0.7	2.2	0.15	3–10	4.5	10–40	1.7×10^{14}	–	–
	TM[b]		9.5	1.6	1.6	0.26	3–5	2.4	20–30	3×10^{13}	–	–
380–420	F		13	2.5	1.5	0.4	5–10	4.5	30–50	2.6×10^{14}	–	–
	TM		15	3.6	1.4	0.5	<5	4.5	30–50	8×10^{13}	–	–
420–460	F		36	35	0.45	1.6	5–20	0.8	–	–	61	9×10^{14}
	TM		47	52	0.20	1.1	10–20	0.35	–	–	50	0.8×10^{14}
350–380	F	~160	12	1	0.28	0.03	–	–	10–100	1.7×10^{15}	–	–
	TM		–	–	0	0	–	–	–	–	–	–
380–420	F		34	30	0.4	1.2	–	–	–	–	62	1.2×10^{15}
	TM		42	45	0.1	0.45	–	–	–	–	–	–
420–460	F		–	–	0	0	–	–	–	–	68	1.2×10^{15}
	TM		–	–	0	0	–	–	–	–	–	–

[a] F – Ferrite.
[b] TM – Tepered martensite.

As the damage dose increased from 100 to ≃140 dpa, the average pore size in ferrite changed from 20 to 24 mm at a constant density of $\sim 1.8 \times 10^{15}$ cm^{-3}. The density of the dislocation network formed in ferrite under irradiation is at a level of 8–10 $\times 10^{10}$ cm^{-2} it which changes slightly within the interval of the specified irradiation parameters. The dislocation density in sorbite is lower. Along with the radiation defects in the irradiated steel microstructure, the formation of fine-dispersion phase, presumably α′-phase, was detected. This process is more intensive in ferrite grains. At a temperature of about 430 °C, the α′-phase concentration is maximum (and the particle size is about 5 nm) [5]. One can assume that at temperatures up to 350 °C the formation processes is slower.

It is typical that in the temperature interval for maximum swelling (Table 1), the α′-phase concentration reduces sharply and the average particle size increases. Of particular note is the formation of a phase of unknown nature (that might be also α′-phase) on void surfaces forming a continuous coating (Fig. 6). The formation is more pronounced in the range 420–430 °C. In sorbite, the process of void decoration with precipitates actually does not take place.

Fig. 7 presents the dose dependence for the maximum change in the diameter of internally pressurized claddings ($\sigma_{max} \approx$ 150–200 MPa) as well as the swelling obtained from the results of structural investigations by TEM. The analysis of the results of the profilometry and electronic microscopy data allows for the following remarks:

- Diameter increase is caused by radiation creep strain and radiation swelling which, on conversion to the diameter increase (6.9 mm), a reaches 0.63% ($\simeq 4.4 \times 10^{-2}$ mm) at 142 dpa;
- The absolute value of strain increment for both increases with increasing damage dose;

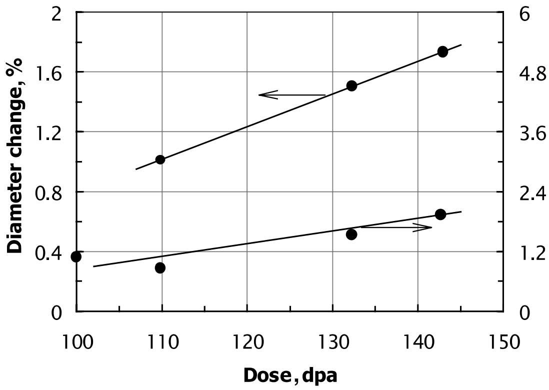

Fig. 7. Dose dependence of the diameter increase and swelling of tubes of steel 0.1C–13Cr–2Mo, V, Nb, B (• – average value of three measurements).

- The strain contribution from swelling in on the total diameter change increases with dose increase from 40% at 110 dpa to ≃60% at 142 dpa.

In order to describe irradiation creep in the temperature range of maximum swelling, an approximation of the following type [11] is used:

$$\frac{\bar{\dot{\varepsilon}}}{\bar{\sigma}} = B_0 + D\dot{S}, \quad (5)$$

where B_0 is the creep modulus, $\mathrm{MPa^{-1}\,dpa^{-1}}$ not depending on dose rate and irradiation temperature; $\bar{\dot{\varepsilon}}$ is the instant creep rate; $\bar{\sigma}$ is the hoop stress in MPa (for tubes with internal pressure $\bar{\sigma} = (\sqrt{3}/2)\sigma_{\mathrm{tang}}$); $\dot{S}$ is the instant an cons swelling rate, $\mathrm{dpa^{-1}}$; D is the relational coefficient for irradiation creep and swelling which reflects the stress influence on swelling and is $(0.7\text{–}1.0) \times 10^{-2}$ $\mathrm{MPa^{-1}}$ [11] for steel HT-9.

Estimations for steel 0.1C–13Cr–2Mo, V, Nb, B ($T_{\mathrm{irr}} = 420\text{–}460$ °C), taking account of measurements (Fig. 7) and assuming that stress $\sigma_{\mathrm{tang}} \approx 200$ MPa, gave the value of coefficient D in the range $(0.3\text{–}0.4) \times 10^{-2}$ $\mathrm{MPa^{-1}}$.

Measurement of the across-the-flats value ΔD and hexagonal tube diagonal ΔS (steel 0.1C–9Cr–1W, V, Ta, B) made it possible to define the irradiation creep and swelling values of steel. Below-core (from −200 to −600 mm), irradiation temperature ≃330 °C, the dose changes from 2 to 26 dpa (Fig. 1) and ΔD increases by 0.1–0.15 mm as compared to the initial size of 44 mm. Estimations of the averaged creep modulus in this region for 10–12 dpa dose using formula (1) gives the following value:

$$B_0 \cong 1.1 \times 10^{-6}\ \mathrm{MPa^{-1}\,dpa^{-1}}.$$

That is 2 times higher than for steel 0.1C–13Cr–2Mo, V, Nb, B.

At levels near core mid plane (up to +200 mm) as a result of irradiation the maximum $\Delta S_{\max}$ and $\Delta D_{\max}$ values are about +80 to +100 mm.

The averaged calculations based on the profilometry data up to a level of about +80 mm (damage dose is ~48 dpa) showed that swelling in this section is no more than 2.3%. The corresponding change in the across-the-flats value is 0.20 mm due to swelling.

Irradiation creep strain was defined from relationship (3) and it reached achieved 0.05–0.09 mm for the selected section. The calculations showed that for ~20 MPa stress in the given section, the coefficient D (Eq. (5)) $\simeq 1 \times 10^{-2}$ $\mathrm{MPa^{-1}}$ for steel 0.1C–9Cr–1W, V, Ta, B. This value agrees with the range of values obtained in experiments by Garner [12]. Definition of swelling in steel 0.1C–9Cr–1W, V, Ta, B by TEM and immersion methods and more exact definition of radiation creep and swelling will make it possible to refine values of coefficients D and B_0 for the investigated compositions of FM steels.

4. Conclusions

Tensile tests were performed for three types of FM steels irradiated to a maximum damage dose of 50 dpa at temperatures ranging from 335 to 540 °C.

1. Differences were identified in the radiation hardening and embrittlement characteristics of steels 0.1C–9Cr–1W, V, Ta, B and 0.1C–12Cr–2W, V, Ti, B and in the manner and mode of failure up to test temperatures of ~420 °C that is attributed to the chromium content and the presence of tantalum in the steel compositions.
2. Yield strength and uniform elongation of steels: 0.1C–9Cr–1W, V, Ta, B; 0.1C–12Cr–2W, V, Ti, B; 0.1C–13Cr–2Mo, V, Nb, B do not differ in the temperature range 420–480 °C and doses from 20 to 50 dpa.
3. Radiation swelling in steels is found beginning at temperatures 410–420 °C and depends on dose and applied stresses. There is a relation between the temperature of void formation and the beginning of the loss of strength of irradiated steels with increasing test temperature.
4. The creep modulus, B_0, and correlation coefficient values for steel 0.1C–9Cr–1W, V, Ta, B are 1.5–2 times higher than similar parameters of steels alloyed with vanadium, molybdenum and niobium. New experiments are required to refine the values of coefficients B_0 and D for W, V, and Ta steels.

References

[1] V.K. Shamardin, A.M. Pecherin, O.M. Vishkarev, V.P. Borisov, G.A. Tulyakov, Proceedings of the International Conference on Radiation Materials Science, vol. 9, Alushta, Kharkov-1991, 22–25 May 1990, p. 3.

[2] D.S. Gelles, Fusion Reactor Materials Semiannual Progress Report for Period Ending 30 September 1992, DOE/ER 03 13/13, 1992, p. 157.

[3] Y. Kohno, A. Kohyama, T. Hirose, M.L. Hamilton, M. Narui, J. Nucl. Mater. 271&272 (1999) 145.

[4] R.L. Klueh, D.J. Alexander, Fusion Materials Semiannual Progress Report for Period Ending, 30 June 1996, DOE/ER-0313/20, Oak Ridge National Lab., 1996, p. 161.

[5] V.K. Shamardin, V.N. Golovanov, T.M. Bulanova, A.V. Povstianko, A.E. Fedoseev, Y.D. Goncharenko, Z.E. Ostrovsky, J. Nucl. Mater. 271&272 (1999) 155.

[6] A.A. Proshkin, L.M. Zabudko, Nekotorye voprosy rabotosposobnosti shestigrannykh chekhlov FA bystrykh reactorov, Reprint IPPE F-701, Obninsk, 1976.
[7] R.L. Klueh, D.J. Alexander, Fusion Materials Semiannual Progress Report for Period Ending, 30 June 1998, DOE/ER-0313/24, Oak Ridge National Lab., 1998, p. 150.
[8] R.L. Klueh, Proceedings on the IEA Working Group Meeting on FM Steels, JAERI Headguarters, Tokyo, Japan, 3–4 November 1997.
[9] A.N. Gubbi, A.F. Rowcliffe, W.S. Eatherly, L.T. Gibson, Fusion Reactor Materials Semiannual Progress Report, DOE/ER-0313/20, 30 June 1996, p. 52.
[10] A. Kimura, M. Narui, T. Misawa, H. Matsui, A. Kohyama, J. Nucl. Mater. 258–263 (1998) 1340.
[11] F.A. Garner, D.S. Gelles, J. Nucl. Mater. 159 (1988) 286.
[12] M.B. Toloczko, F.A. Garner, G.R. Eiholzer, J. Nucl. Mater. 258–263 (1998) 1163.